a NASA facsimile reproduction

OF

N65-21000

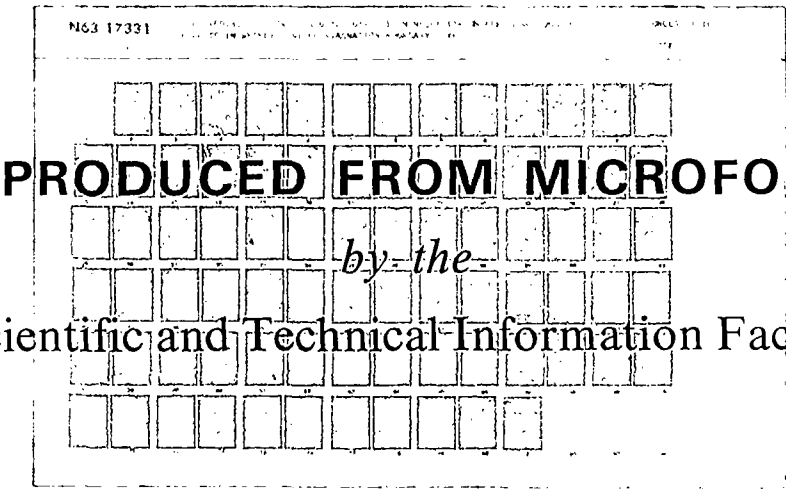

REPRODUCED FROM MICROFORM

by the

Scientific and Technical Information Facility

NASA TECHNICAL MEMORANDUM

NASA TM X-53216

MARCH 12, 1965

NASA TM X-53216

THE SOLAR FLARE ENVIRONMENT

by W. T. ROBERTS
Aero-Astrodynamics Laboratory

NASA

George C. Marshall Space Flight Center, Huntsville, Alabama

TECHNICAL MEMORANDUM X-53216

THE SOLAR FLARE ENVIRONMENT

By

W. T. Roberts

George C. Marshall Space Flight Center

Huntsville, Alabama

ABSTRACT

Of all the natural environments of extraterrestrial space, probably the most hazardous is the radiation to be encountered. The three main sources of radiation are galactic cosmic rays, Van Allen belt particles, and solar flare particles. Galactic cosmic rays are very high energy particles, but since their flux is low, they will not be considered in this analysis. The Van Allen belt particles will not be considered, since we are specifically interested in the environment encountered at some distance from earth greater than about fifteen earth radii. Thus, we are left with the solar flare as the main contributing source of intensive radiation.

Discussed is the solar atmosphere including the photosphere, chromosphere, and corona. Most of the main structures found within these areas are mentioned, and some are elaborated on.

Next are described the various types of solar flares which have be observed. The problem of constructing a solar flare "model" is discus and percentile curves based on presently available data are suggested a solution. These curves are drawn for the 99.9 percentile, 50 percen 67 percentile, and 50 percentile groups.

Probabilities of solar flare occurrence, and methods now being use as a basis for studies on solar flare predicting are considered. It i concluded that even accurate solar flare predictions cannot alleviate the amount of shielding required for a long duration extraterrestrial mission.

A few of the complications involved in solar flare shielding calculations are covered, and a possible means of approach to these probl is suggested for future extraterrestrial missions.

NASA - GEORGE C. MARSHALL SPACE FLIGHT CENTER

NASA - GEORGE C. MARSHALL SPACE FLIGHT CENTER

Technical Memorandum X-53216

March 12, 1965

THE SOLAR FLARE ENVIRONMENT

By

W. T. Roberts

SPACE ENVIRONMENT GROUP
AEROSPACE ENVIRONMENT OFFICE
AERO-ASTRODYNAMICS LABORATORY
RESEARCH AND DEVELOPMENT OPERATIONS

5

TABLE OF CONTENTS

6

LIST OF ILLUSTRATIONS

THE SOLAR FLARE ENVIRONMENT

SUMMARY

Of all the natural environments of extraterrestrial space, probably the most hazardous is the radiation to be encountered. The three main sources of radiation are galactic cosmic rays, Van Allen belt particles, and solar flare particles. Galactic cosmic rays are very high energy particles, but since their flux is low, they will not be considered in this analysis. The Van Allen belt particles will not be considered since we are specifically interested in the environment encountered at some distance from earth greater than about fifteen earth radii. Thus, we are left with the solar flare as the main contributing source of intensive radiation.

Discussed is the solar atmosphere including the photosphere, chromosphere, and corona. Most of the main structures found within these areas are mentioned, and some are elaborated on.

Next are described the various types of solar flares which have been observed. The problem of constructing a solar flare "model" is discussed, and percentile curves based on presently available data are suggested as a solution. These curves are drawn for the 99.9 percentile, 90 percentile, 67 percentile, and 50 percentile groups.

Probabilities of solar flare occurrence, and methods now being used as a basis for studies on solar flare predicting are considered. It is concluded that even accurate solar flare predictions cannot alleviate the amount of shielding required for a long duration extraterrestrial mission.

A few of the complications involved in solar flare shielding calculations are covered, and a possible means of approach to these problems is suggested for future extraterrestrial missions.

I. INTRODUCTION

One of the many problems which must be coped with before extraterrestrial missions become routine is that of radiation hazards. Even though very little is certain about the radiation environment in space today - scarcely five years before the first scheduled landing of men on the lunar surface - our knowledge has increased by many orders of

magnitude over what we even suspected a few years ago. One can only hope that this gradient of data collection and interpretation can be maintained so that the success of this lunar mission and all succeeding extraterrestrial missions may surmount the natural radiation problem.

The solar flare with its associated proton event has been studied for only a few years. Before 1956 the main source of particulate radiation outside the earth's atmosphere was assumed to be from galactic cosmic rays. These particles are found to bombard the earth with individual energies ranging from a few Mev up to as much as 10^9 Bev. At several times during the earlier years, large increases were noted on ground-based recorders of the cosmic ray intensity. These increases are now believed to have resulted from solar flare proton events. With the advent of high altitude balloons, rocket probes, and satellites, much more data have become available about solar flares.

Flares are usually associated with active centers on the sun. These active regions are made up of sunspot groups which are relatively dark spots appearing on the photosphere - the visible surface. Sunspots are regions of intensive magnetic fields on the sun, with field intensities in the kilogauss range. These regions are cooler than the surrounding photospheric temperatures of about 6000°K. These cooler temperatures are caused by the impedance of charged particle flow by the intense magnetic fields. The exact mechanisms involved in the solar proton events are not yet well understood, but a number of interesting studies are now underway, some of which will be discussed in the following sections.

II. THE SOLAR ATMOSPHERE

Before proceeding into the actual solar flare environment model itself, it might be helpful to identify some features and terms used in solar studies. The sun is actually a dwarf star which belongs to a class common in the galaxies.

The photosphere is the visible disk of the sun from which most of the electromagnetic radiation is emitted. Since it is made up of an opaque gas approximately 350 kilometers in depth, it is considered a part of the solar atmosphere rather than the surface of the sun. The temperature of the photosphere ranges from about 8000°K at the bottom to 4500°K at the top. The wavelength-intensity curve fits closely the curve emitted by a 6000°K black body (Figure 1) between wavelengths 1000 Å to 1 cm [18].

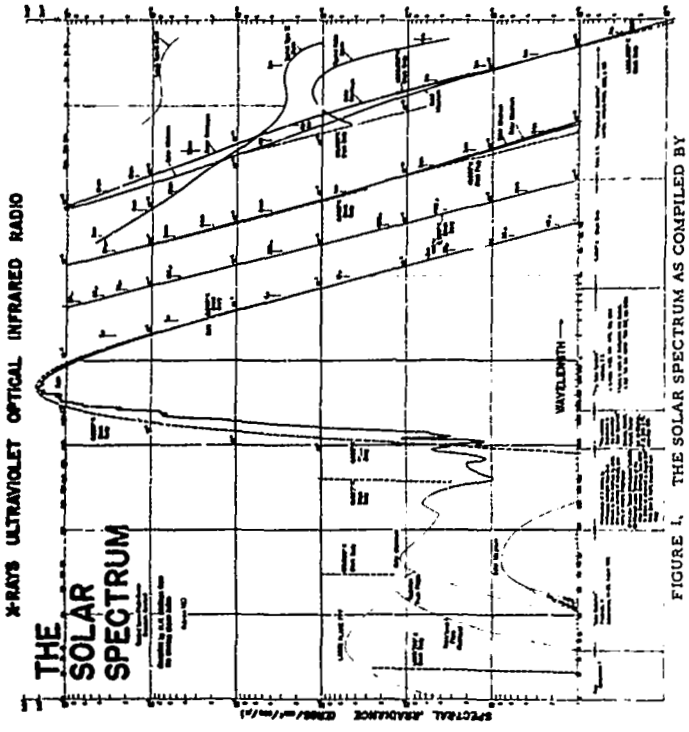

FIGURE 1. THE SOLAR SPECTRUM AS COMPILED BY H. H. MALITSON, FEBRUARY 1963

The photosphere when magnified is observed to have a granular structure rather than a smooth surface. This configuration is one of small bright cell-like structures several hundred kilometers in diameter separated by darker and cooler areas. The "granules" have a mean life of from three to six minutes and are the results of convection in the photosphere.

The chromosphere is the transition region between the 6000°K photosphere and the 2,000,000°K corona. The chromosphere rises to a height of several thousand kilometers above the photosphere and is spicular in appearance. The spicules, which appear as bright spikes sticking out of the photosphere, are apparently the result of cool and hot columns of material flowing through this region. The spicules are thought to be cooler than the surrounding regions. The exact manner in which this region of the solar atmosphere conducts heat to the corona remains to be explained.

The corona, as mentioned earlier, is the sun's outermost atmosphere. It extends from just above the chromosphere out beyond the earth's orbit, and; according to some observations, may not terminate by recombination until beyond the orbit of Mars. The temperature of the corona is estimated as being about 2,000,000°K with a variation directly proportional to the solar activity. The density of the corona is very tenuous thus making the tremendous temperature of little concern in space flight engineering. The corona is also the region within which the solar wind exists. The solar wind velocities as measured by Mariner II range from 300 to 600 kilometers per second with a density of 2 to 20 particles per cubic centimeter [1].

Filaments and prominences are apparently two names for the same phenomenon. The prominence is observed on the limb against a dark sky and thus appears bright, whereas the filament is seen against the solar disc and appears to be a dark thread across the photosphere. The structures are actually long thin sheets of gas rising above the chromosphere to heights of about 40,000 kilometers.

Solar bursts refer to large increases in intensity of the radio noise emissions from the sun, lasting from a few seconds to a few minutes. Table I and Figure 2 depict the radio frequency history of a solar flare

Faculae, which are dark regions appearing on the photosphere and extending into the chromosphere, are largely associated with sunspot groups and exhibit the same variation with solar activity. The bright areas, located in the chromosphere, but associated with the faculae, have been called plage regions or flocculi. In general, the faculae and plage will develop rapidly and associated sunspots appear shortly thereafter; however, the sunspot will disappear long before the plage has completely faded out.

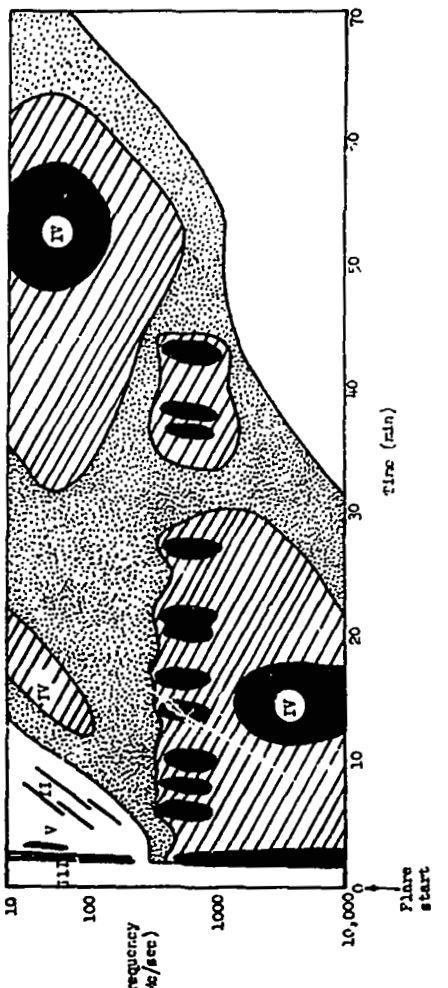

FIGURE 2. TIME-RADIO FREQUENCY DIAGRAM OF A SOLAR FLARE (See Table I)

TABLE I

CHARACTERISTICS OF SOLAR NOISE

Type	Identifying Characteristics	Source Characteristics	Frequency Characteristics
I	Noise storms usually lasting from hours to days; or bursts of ~ 1 second duration.	Assumed to be of a non-thermal origin, associated with sunspots, "R centers," and sometimes flares.	Less than ~ 250 Mc/sec with bandwidth 1-10 Mc/sec for bursts and 10-100 Mc/sec for continuum. The intensity at 100 Mc/sec 10^{-21} - 10^{-19} $\frac{\text{watts}}{\text{m}^2\text{(c/sec)}}$
II	Bursts with slow drift of ~ -0.3 Mc/sec^2 lasting from 5-10 minutes.	Source is due to plasma oscillations associated with flares. Occurrence begins about 7 minutes after flare. The source moves outward at ~ 1000 km/sec.	Mainly less than 150 Mc/sec with the bandwidth of about 2×10^{-1} of the observed frequency. Intensity at 100 Mc/sec is usually 10^{-20} to 10^{-19} $\frac{\text{watts}}{\text{m}^2\text{(c/sec)}}$
III	Bursts with fast drift of ~ 30 Mc/sec^2 lasting singly 3-10 sec or in groups of 1-5 minutes.	Assumed to be associated with plasma oscillation associated 50-60% of the time with flares. The source has an outward velocity of ~ 10^5 km/sec.	Ranges from > 4000 Mc/sec to < 10 Mc/sec with a bandwidth almost equal to the frequency. The intensity usually is less than 10^{-20} $\frac{\text{watts}}{\text{m}^2\text{(c/sec)}}$
IV	Smooth continuum lasting from minutes to hours.	Source is due to synchrotron radiation. Occurring 70-80% of the time with flares at ~ 15 minutes after start. Initial source velocity ranges from 1-5 x 10^5 km/sec for about 10 minutes and then source becomes stationary.	Cover the complete radio band but vary from burst to burst. The bandwidth is frequently several octaves with intensities from 10^{-20} to 10^{-19} $\frac{\text{watts}}{\text{m}^2\text{(c/sec)}}$

TABLE I (Continued)

Type	Identifying Characteristics	Source Characteristics	Frequency Characteristics
V	Smooth continuum lasting from 1-2 minutes.	Synchrotron radiation occurring before the maximum of solar flares. The velocity of the source is ~ 5 x 10^3 km/sec.	Frequencies less than 200 Mc/sec with a bandwidth of several Mc/sec at 50-100 Mc/sec. Intensities 10^{-20} to 10^{-19} $\frac{\text{watts}}{\text{m}^2\text{(c/sec)}}$
Micro-wave	Continuum and bursts lasting 0.5 to 20 minutes.	Assumed to be of synchrotron and possibly thermal origin associated about 80% of the time with flares.	The frequency range is ~ 1000-20,000 Mc/sec with a bandwidth of several octaves. The intensity is usually ~ 5 x 10^{-22} to 5 x 10^{-20} $\frac{\text{watts}}{\text{m}^2\text{(c/sec)}}$ at 3000 M/sec.

Of all the previously mentioned structural features of the sun, none are as well known and documented as the sunspots. Sunspots are areas of intensive magnetic fields which inhibit the outward flow of gases in the photosphere. They usually consist of at least one positive pole and at least one negative pole, but sometimes occur with only one polarity in all the spots. Generally, the east-west polarity of the fields places one particular pole (either positive or negative) in a given hemisphere for each bipolar sunspot group preceding the other pole for all sunspots in that hemisphere. In the opposite hemisphere, the polarity is reversed for all bipolar sunspot groups. At sunspot minimum, which occurs about every eleven years, this polarity situation reverses for each hemisphere.

Because these intensive magnetic fields inhibit plasma flow, sunspots are cooler regions than the surrounding photosphere. Sunspot groups can have areas up to .55 percent of the visible solar disk and perhaps more. They consist of a dark center area called an umbra and a brighter (but still dark when compared to the photospheric brightness) penumbral area.

There are three time characteristics normally used to describe solar flares:

(a) the onset delay time, the time from maximum optical emission by the flare on the sun to the arrival of the first particles at the earth;

(b) the rise time, defined as the time between the arrival of the first flare particles and the time of maximum flux intensity;

(c) the decay time, or the time required for the particle flux to decrease from maximum intensity to the normal preflare background.

Each of these three time characteristics may be applied to individual flares, or they may be applied to groups of particles, each group having a specific energy or energy range for the particles contained therein. Regardless of how they are applied, they vary from flare to flare.

Flares are observed on the solar surface as being sudden increases in light intensity, especially in the H_α spectral line at 6563 A. They are almost always associated with sunspot groups, and are assumed to result from the catastrophic expulsion of high energy particles.

III. FLARE MODEL

The term "flare model" is actually a misnomer since each flare is individual in time and energy. There are various aspects which cause these differences, some of which will be elaborated on later. Figure 3 is a plot of the energy spectrum of three different large flares.

Normally, the flux of particles over 100 Mev is a fairly small percentage of the flux of particles over 30 Mev; however, for the February 23, 1956 flare, the number of particles whose energies exceeded 100 Mev was 35 percent of the number of particles whose energies exceeded 30 Mev. This means that this particular flare had a large number of high energy particles. The number of particles over 10 Mev was 1.8×10^9 where 1.0×10^9 or over 50 percent were over 30 M[illegible] July 14, 1959, there was a solar flare whose total flux of part[illegible]ch energies greater than 10 Mev was 7.5×10^9 or over four tim[illegible]reat as the flux of the February 23, 1956, event; however, the flu[illegible] of particles with energies over 100 Mev was less than one third of the February 23, 1959 event. These two flares are examples of high energy flares and low energy flares, respectively. The high energy flares appear to have lower total number of particles, but the energies are much higher and

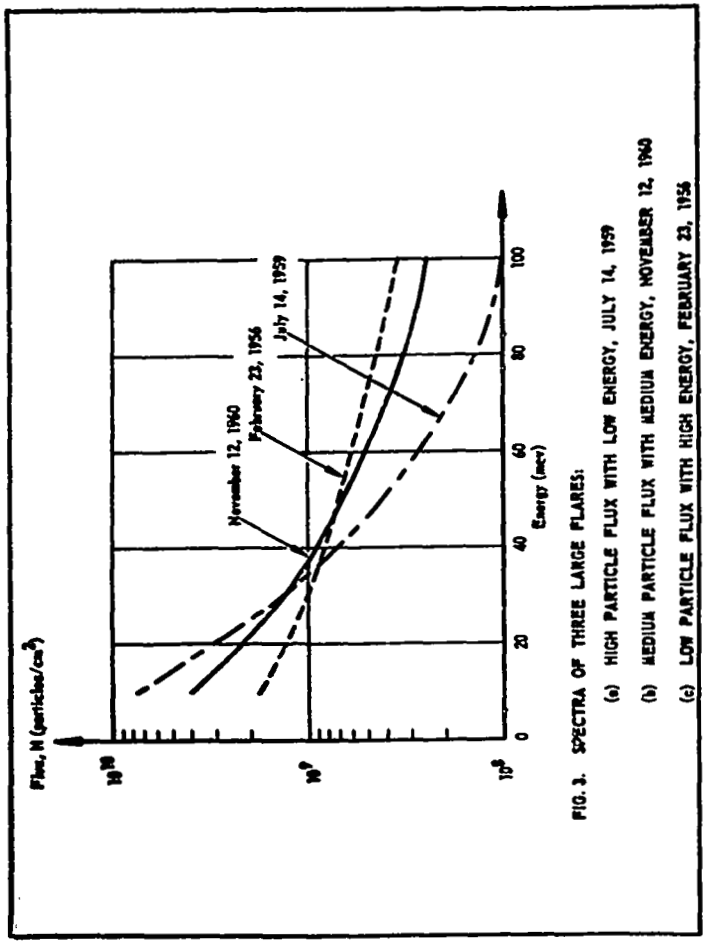

FIG. 3. SPECTRA OF THREE LARGE FLARES:
(a) HIGH PARTICLE FLUX WITH LOW ENERGY, JULY 14, 1959
(b) MEDIUM PARTICLE FLUX WITH MEDIUM ENERGY, NOVEMBER 12, 1960
(c) LOW PARTICLE FLUX WITH HIGH ENERGY, FEBRUARY 23, 1956

therefore require much thicker shielding. Still a third type of flare is intermediate between the July 14, 1959 and the February 23, 1956 type flares. This is depicted by the November 12, 1960 flare. In this flare, the flux of particles with energies between ~ 30 Mev and ~ 48 Mev exceeded either of the other two flares previously discussed.

The parameter, P_o, the rigidity of particles, is one method by which high energy particles are often classified. P_o is determined by the formula

$$P_o = C\sqrt{\frac{(m^2 - m_o^2)\, C^2}{ze}}$$

where

m = particle relativistic mass

m_o = particle rest mass

C = velocity of light

ze = total charge on the particle.

This formula may be reduced to the form

$$P_o = \frac{\sqrt{(E + m_o C^2)^2 - (m_o C^2)^2}}{ze}$$

where E is the total particle energy.

In this form, one may substitute the particle Mev energy for E and obtain the particle rigidity directly from the particle energy. If E is in Mev, the rigidity is given in million volts or Mv. If E is in Bev, then the rigidity is in Bv or billion volts, and so forth. In each case, of course, the term $m_o C^2$ is the particle rest energy expressed in appropriate units. Table II is a compilation of some flares and their respective rigidities by Webber, et al. [2].

TABLE II

INTEGRAL FLUX AT 10, 30, and 100 MEV AND CORRESPONDING CHARACTERISTIC RIGIDITY P_o

Date	J(> 10 Mev)	J(> 30 Mev) (protons/cm^2)	J(> 100 Mev)	P_o (MV)
2/23/56	1.8×10^9	1.0×10^9	3.5×10^8	195
3/11/56	-	-	-	-
8/3/56	-	2.5×10^7	6×10^6	144
11/13/56	-	-	-	-
1/20/57	-	2×10^8	7×10^7	61
4/3/57	-	-	-	-
6/22/57	-	-	-	-
7/3/57	-	2×10^7	-	-
8/9/57	-	1.5×10^6	-	-
8/29/57	-	1.2×10^8	3×10^6	56
9/21/57	-	1.5×10^6	-	-
10/20/57	-	5×10^7	1×10^7	127
11/4/57	-	9×10^6	-	-
2/9/58	-	1×10^7	-	-
3/23/58	2×10^9	2.5×10^8	1×10^7	64
4/10/58	-	5×10^6	-	-
7/7/58	1.8×10^9	2.5×10^8	9×10^6	62
8/16/58	4×10^9	4×10^7	1.6×10^6	64
8/22/58	8×10^8	7×10^7	1.8×10^6	56
8/26/58	1.5×10^9	1.1×10^8	2.0×10^6	51
9/22/58	9×10^7	6×10^6	1×10^5	50
5/10/59	5.5×10^9	9.6×10^8	8.5×10^7	84
6/13/59	-	8.5×10^7	-	-
7/10/59	4.5×10^9	1.0×10^9	1.4×10^8	104
7/14/59	7.5×10^9	1.3×10^9	1.0×10^8	80
7/16/59	3.3×10^9	9.1×10^8	1.3×10^8	105
8/18/59	-	1.8×10^6	-	-
1/11/60	-	4×10^5	-	-
5/1/60	1.5×10^7	5.0×10^6	8.5×10^5	116
4/5/60	-	1.1×10^6	-	-
4/28/60	1.3×10^7	5.0×10^6	7×10^5	104
4/29/60	-	7×10^6	-	-
5/4/60	1.2×10^7	6×10^6	1.2×10^6	127
5/6/60	-	4×10^6	-	-
5/13/60	1.5×10^7	4×10^6	4.5×10^5	94

TABLE II (Continued)

Date	J(> 10 Mev)	J(> 30 Mev) (protons/cm^2)	J(> 100 Mev)	P_o (Mv)
6/1/60	-	4×10^5	-	-
8/12/60	-	6×10^5	-	-
9/3/60	9×10^7	3.5×10^7	7×10^6	127
9/26/60	2×10^7	2.0×10^6	1.2×10^5	73
11/12/60	4×10^9	1.3×10^9	2.5×10^8	124
11/15/60	2.5×10^9	7.2×10^8	1.2×10^8	114
11/20/60	1.4×10^8	4.5×10^7	8×10^6	118
7/11/61	1.7×10^7	3×10^6	2.4×10^5	81
7/12/61	5×10^8	4×10^7	1×10^6	56
7/18/61	1×10^9	3×10^8	4×10^7	102
7/20/61	1.5×10^7	5×10^6	9×10^5	120
7/28/61	5×10^7	6×10^6	1.1×10^6	121
11/10/61	5×10^7	6×10^6	1.1×10^6	121
2/4/62	-	-	-	-
10/23/62	6×10^5	1.2×10^5	1×10^4	83

After studying the various solar flare flux and energy distributions, it is apparent that no model flare can be derived which will account for all the flare spectrums. Possibly the most reasonable approach is to derive a maximum "envelope" which covers all the flares thus far studied and use this for our extreme design purposes.

Such a model will necessarily include a maximum flux in each energy region studied. The resulting total dose calculated from such a model will be high, but the probability of exceeding such a flare spectrum will be very low. It is thus suggested that the solar flare model adopted be determined directly from data which exist on the presently available solar flare spectra.

Figure 4 represents one approach to the solar flare energy-flux solution. Curve A represents the maximum envelope for all solar flares. It is devised by taking the maximum flux in the 10, 30, and 100 Mev energy ranges. Although this curve represents an ideal design curve, it is obvious from a look at the shielding required for this flux of particles that vehicle protection would be impossible with present day shielding characteristics. Almost 5 grams/cm^2 of shielding is required just to reduce the dose to 100 rads. Curve B on the other hand is a more realistic approach. This curve covers approximately 90 percent

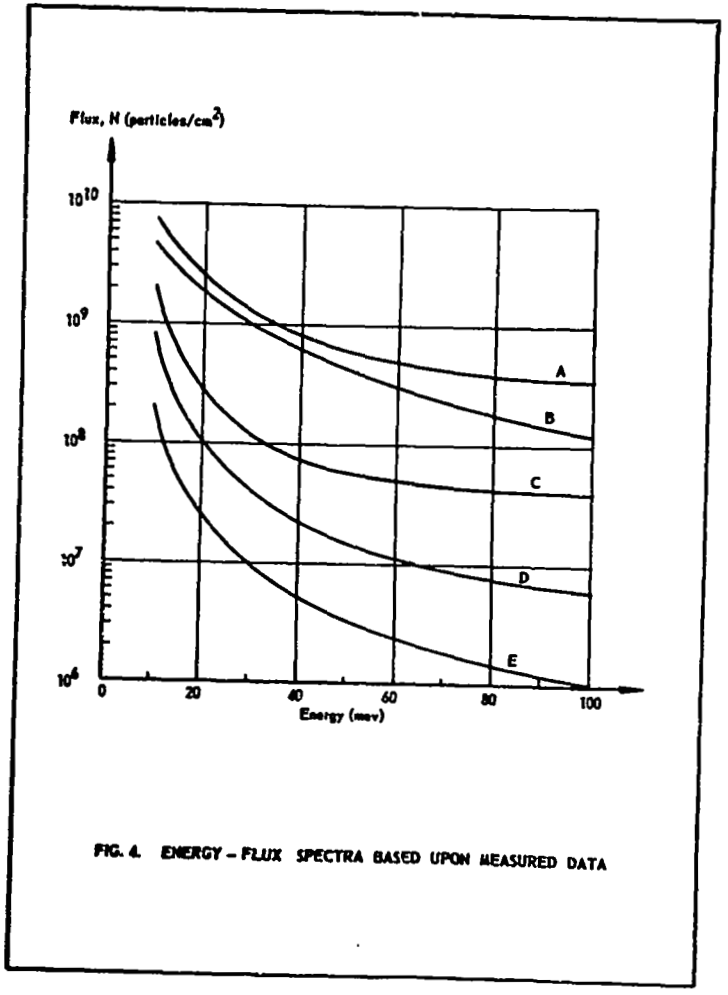

FIG. 4. ENERGY – FLUX SPECTRA BASED UPON MEASURED DATA

of the flares with fluxes over 10^3 in the 10, 30, and 100 Mev ranges. This flare spectrum would reduce the shielding requirement by about 20 percent. Curve C covers two-thirds of the flares over 10^5 in flux. The big factor here is that less than 2 grams/cm^2 is required to reduce the radiation to less than 100 rads, and at 5 grams/cm^2 the dose is only about 20 rads. Curve D is a fifty percent curve for flares that have flux over 10^9 particles/cm^2, and curve E is arbitrarily chosen to represent the minimum flux-energy spectrum which should be even considered.

Each of these curves was obtained by taking the existing flare data and calculating which flare in the individual energy ranges - 10, 30, and 100 Mev - had the given percentage of flares under it.

The development of a typical solar flare in time is shown in Figure 5. The earliest arriving particles are near relativistic in energy, and their flux is anisotropic, usually appearing to originate at about 50° west of the sun. This means that the particle energies are large enough that their distribution is not severely affected by the ambient solar magnetic field.

The energies associated with these particles are in the Bev range, and the particles themselves are mostly protons. However, Freier and Webber [3] have recently completed a study of radio-absorption measurement which indicates that above a certain rigidity, the ratio of protons to alpha particles is 1:1 for several flares. Table III is a listing of a few flares with their associated proton to alpha ratios and rigidities.

TABLE III

Date	J_p/J_α	P_0(Mv)
February 23, 1956	1	195
May 10, 1959	1	84
July 10, 1959	1	104
July 14, 1959	1	80
September 3, 1960	30	127
November 12, 1960	1	127
November 15, 1960	2	114
July 12, 1961	1	56
July 18, 1961	6	102

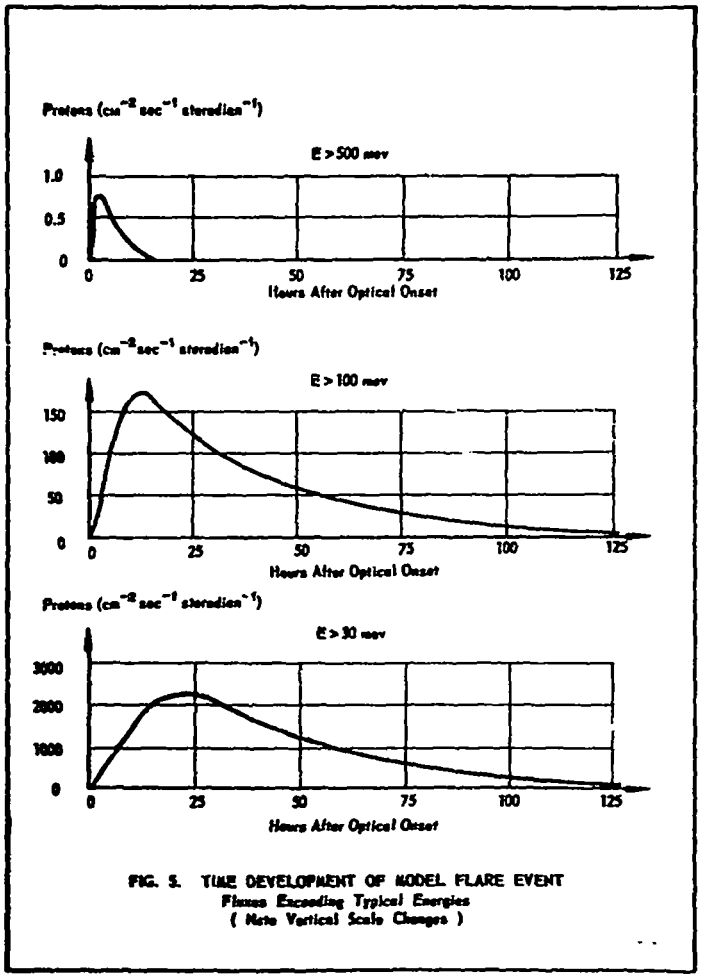

FIG. 5. TIME DEVELOPMENT OF MODEL FLARE EVENT
Fluxes Exceeding Typical Energies
(Note Vertical Scale Changes)

The flux of these very high energy particles is very small when compared to the integrated flare flux itself, but from a radiation point of view these particles are far more important. Table IV shows the range of protons in aluminum as an illustration:

TABLE IV

RANGE OF PROTONS IN ALUMINUM

Energy (Mev)	Range (gm/cm^2)
1	.0035
10	.17
100	10.5

The rise time associated with these particles is very short, on the order of one-half hour for the highest energy particles.

On the other hand, the decay time is also short, relative to the lower energy particles. As can be seen from Figure 5, the normal decay time for particles with energies over 500 Mev is on the order of 16 hours, whereas the decay time for particles of energies over 100 Mev is several days.

As time increases, the lower energy, more intensive flux reaches the earth, and the particles become completely isotropic in distribution due to the scattering of the particles by diffusion through the solar magnetic field. This plasma flow is a completely ionized, and therefore a highly conducting medium; thus, as it expands outward from the solar surface, the plasma takes with it some of the surrounding magnetic field. This expanding magnetic field intensifies the normal field strength of the region occupied by the plasma flow with the result that the normal cosmic ray intensity within the region is decreased due to the stronger deflection of particles. This phenomenon is known as the Forbush decrease. On earth it appears as a decrease in the cosmic ray flux found to occur just before a magnetic storm.

When the expanding plasma cloud encounters the earth's magnetosphere, there is a resulting compression and deformation of the geomagnetic field. There is also an enhancement of the earth's ring current, due to the ionized particles flowing into these regions from the poles. The two situations combine to cause a geomagnetic storm and the associated auroral display.

The plasma cloud continues to expand until an equilibrium condition is reached where the particle flux is equal in all directions.

IV. SOLAR FLARE PROBABILITIES AND PREDICTING

Two methods were used to calculate the probabilities, p, of occurrence of solar flares. One was the standard n_f/n_t method shown in Figure 6. Of a total number of days, n_t, there were n_f occurrences of flares whose individual total integrated flux exceeded the vertical scale.

The objection to this type of analysis is that the data presently available might not warrant this n_f/n_t relation. The alternative then might be to assume a Poisson distribution and choose instead an equation used by Dalton [34] to calculate meteor parameters.

$$p = 1 - \left[\frac{(1 - C)}{e^{n_f}}\right]^{[(3+2C)/4]^{\delta}/(n_t - n_f)/2)}$$

where

$\delta = 0$ when $n_f = 0$

$\delta = 1$ when $n_f \neq 0$

C = confidence that the probability of event occurrence per trail is not greater than p. Here C = 1/2.

Therefore,

$$p = 1 - \left[\frac{1}{2e^{n_f}}\right]^{1/(n_t - n_f/2)} .$$

At this point, we notice that flares tend to group themselves. This is to say that, if one flare occurs, the following few days have a higher probability of flare occurrence than otherwise. Looking back at Table II, we notice in particular August 1958, July 1959, April 1960, May 1960, November 1960, and July 1961.

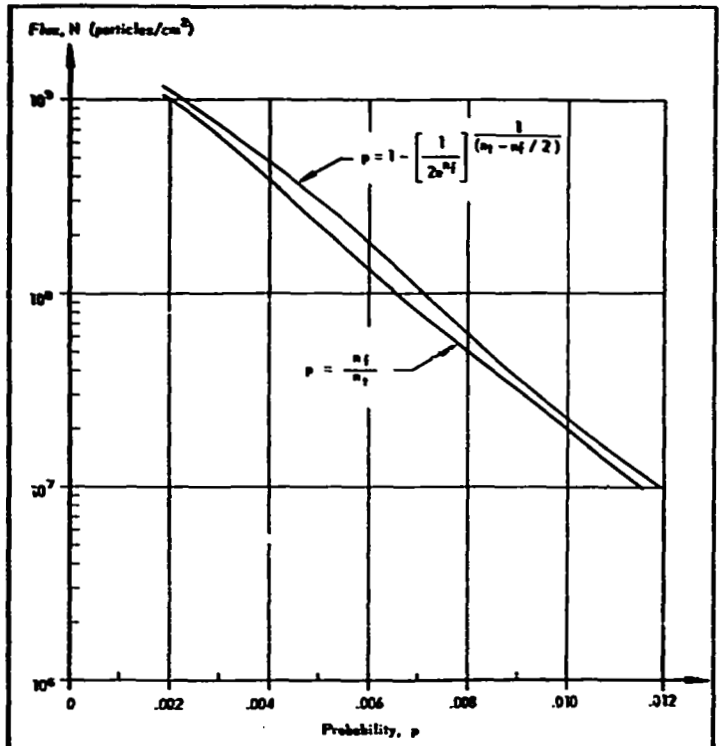

FIG. 6. THE PROBABILITY, p, OF THE OCCURRENCE OF A FLARE WHOSE FLUX IS EQUAL TO OR GREATER THAN N, AND WHOSE INDIVIDUAL PARTICLE ENERGIES ARE EQUAL TO OR GREATER THAN 30 MEV

Long range predicting of the occurrence of solar flares is one of the major undertakings for insuring safety of extraterrestrial missions. A number of studies have been and are being made to establish reliable means of predicting solar flare occurrences. Some of these studies and observations will now be discussed.

It is generally assumed that solar flares are associated with sunspots which generate at least a part of the energy required for the event occurrence. However, there are examples of solar flares occurring at points where no sunspots appeared to exist. Since these occasions are rare, a relatively obvious way of approaching the solar flare prediction problem is to study the sunspots and sunspot groups themselves.

Anderson [35] has pointed out the apparent correlation between large penumbral areas of sunspots and the subsequent occurrence of a solar flare. The criterion which Anderson used was that large unbroken penumbral areas must equal or be greater than the area of the July 5, 1958, penumbral region. He also restricted to two the number of spots in a group that could contribute to this criterion. In the three-year period studied, out of a total of forty events observed, only two occurred outside of a time period when these large penumbral areas were observed. Furthermore, it was found that for the events which did occur when large penumbral areas were observed, none occurred before two days after the development of a "critical" penumbral size. The data for this study were collected over a three-year period, which is a very short time when measured in astronomical studies. The next solar cycle should provide data on the validity of this theory.

In addition to the sunspot correlation, it has been observed for some time by a number of people that the times of minimum and maximum solar activity seem to be relatively free from solar flare occurrences. Rather, the solar flares tend to occur on the rising or falling slope of solar activity. Once again, this could be a real effect or it could be a coincidence, but if the effect is real, it may mean that we will perform our manned extraterrestrial - or better, extramagnetospheric - missions during sunspot maximum and minimum, and concentrate on earth orbiting and unmanned extramagnetospheric missions at in-between times.

Most of the high energy events have also been observed to have had their optical flares on the western limb of the sun. This is probably due to the trajectories followed by the high energy particles. Apparently, the path to the earth's orbit is more nearly open to particles originating on the west limb of the sun.

As was mentioned earlier, sunspots which have had a previous flare are more likely to have another flare than a sunspot with no flare history. There is also some evidence to indicate that the first flare might tend to "open" the way for subsequent flares in the interplanetary medium. For instance, in a series of flares from the same region, the first seems to clear the way for the following flare or flares. The subsequent flare particles tend then to be more intense, as if they were funneled along after the primary flare.

Guss [6] has performed a study of the distribution of flares which produce particles at the earth with heliographic longitude. His graph, Figure 7, shows that at 90 degrees heliographic longitude there is a tremendous increase in the number of detected events. This is especially true with the monitoring of the high energy particles.

In still another case, the "seasonal" occurrence of solar flares is being studied. In the time periods of December 3 to January 15 and May 15 to July 8, only one solar particle event has been recorded. The only immediate apparent correlation here is that, during the early part of June and December, the earth crosses the sun's equator. It is conceivable that because of the reversal of magnetic poles in the opposite hemispheres, a region of magnetic turbulence is established so that in that region there is a dearth of solar flare particles. Figure 8 is a graph showing this effect.

The final program for solar flare prediction of which the author is aware is an attempt to correlate solar flares with planetary alignment. If one could establish that the gravitational effects of the planets do significantly perturb the innermost reaches of the sun, then one might imagine that solar flares could be correlated with planetary alignments.

When all of these theories and study results are combined, it develops that missions should be planned for December or May just after the 90 degree heliographic meridian has passed behind the limb, during a time when there are no sunspots with large unbroken penumbral areas (or if there are, they should not be located on the west limb), at a time of maximum or minimum solar activity, and when the planets are evenly distributed around the sun.

The serious problem develops when one considers extraterrestrial missions planned for the next ten years. These missions will be extremely limited if the mission lengths have to be restricted to times when solar flares are unlikely to occur. This throws the main burden of protection right back on the radiation shielding employed.

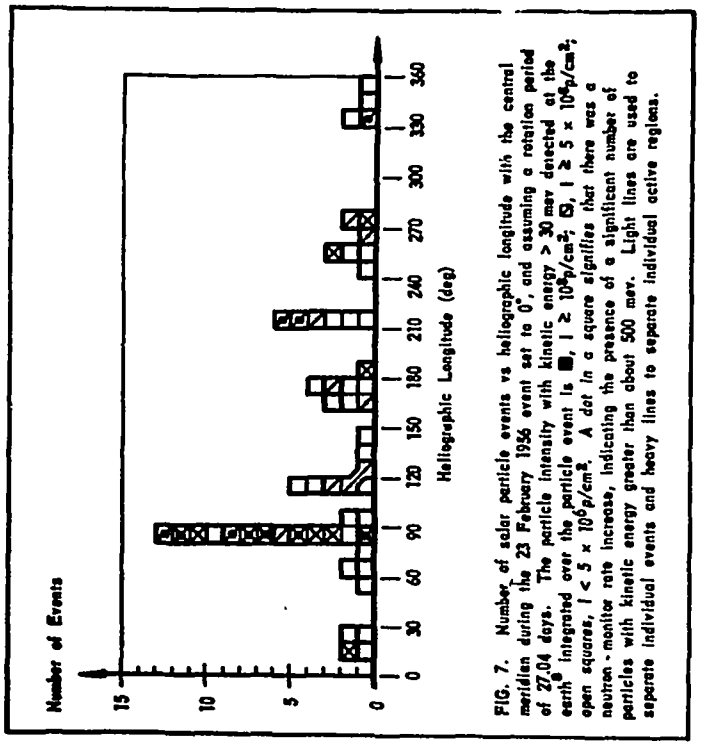

FIG. 7. Number of solar particle events vs heliographic longitude with the central meridian during the 23 February 1956 event set to 0°, and assuming a rotation period of 27.04 days. The particle intensity with kinetic energy > 30 mev detected at the earth integrated over the particle event is ■, $I \geq 10^8$ p/cm², ▨, $I \geq 5 \times 10^8$ p/cm², open squares, $I < 5 \times 10^8$ p/cm². A dot in a square signifies that there was a neutron-monitor rate increase, indicating the presence of a significant number of particles with kinetic energy greater than about 500 mev. Light lines are used to separate individual events and heavy lines to separate individual active regions.

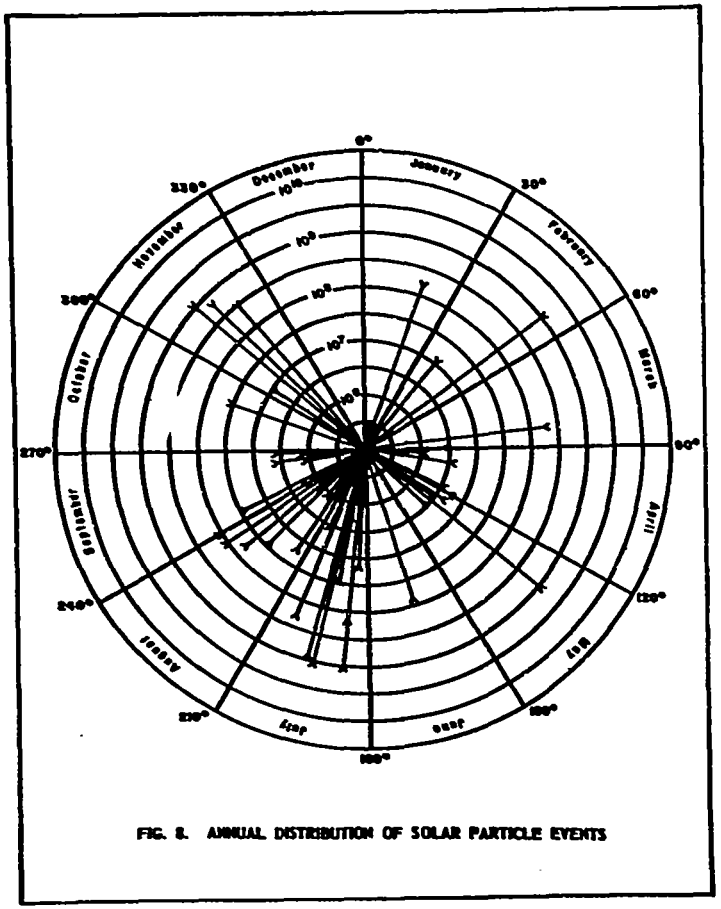

FIG. 8. ANNUAL DISTRIBUTION OF SOLAR PARTICLE EVENTS

V. CONSIDERATIONS FOR SOLAR FLARE SHIELDING

In performing shielding calculations, one should first establish the amount of radiation which might be called the maximum allowable. To specify a shielding criterion for the human organism, we specify an LD_{50}, or the dose in rads which would be lethal to 50 percent of the population in 30 days. The LD_{50} for a skin dose is generally considered to be about 500 rads distributed evenly over the whole body. When speaking of organs of the body, one specifies the LD_{50} as the radiation dose which will cause the specific organ to cease functioning in 50 percent of the population. For the blood-forming organs, this point is 200 rads, and for the eyes, the dosage is often considered to be 100 rads.

The difference here comes from the fact that the cells of certain organs are essentially irreplaceable. The cellular structures within the eye are good examples of this; thus, we say that the relative biological effectiveness, RBE, for the eyes is large. On the other hand, the RBE for the extremities, hands and feet, is low.

The following table is a compilation by Tobias [19] of the expected effects of human acute whole-body radiation exposure given in roentgens.

TABLE V

Acute Dose (Roentgens)	Probable Effect
0-50	No obvious effect, except possibly minor blood changes.
80-120	Vomiting and nausea for about 1 day in 5 to 10 percent of exposed personnel. Fatigue, but no serious disability.
130-170	Vomiting and nausea for about 1 day, followed by other symptoms of radiation sickness, in about 50 percent of personnel. No deaths anticipated.
270-330	Vomiting and nausea in nearly all personnel on the first day, followed by other symptoms of radiation sickness. About 20 percent deaths within 2 to 6 weeks after exposure; survivors convalesce for about 3 months.
400-500	Vomiting and nausea in all personnel on the first day, followed by other symptoms of radiation sickness. About 50 percent deaths within 1 month; survivors convalesce for about 6 months.

TABLE V (Continued)

Acute Dose (Roentgens)	Probable Effect
550-750	Vomiting and nausea in all personnel within 4 hours of exposure, followed by other symptoms of radiation sickness. Up to 100 percent deaths. Any survivors convalesce for about 6 months.
1000	Vomiting and nausea in all personnel within 1 to 2 hours. Probably no survivors from radiation sickness.
5000	Incapacitation almost immediately. Fatal to all personnel within one week.

Another term, other than RBE, which is normally used to express the amount of radiation imposed upon a structure is the LET. The LET or linear energy transfer is a measure of the amount of energy transferred from the radiating particle to the irradiated material as the particle passes through a standard thickness. The LET value then varies with material irradiated, the radiating particle's energy, and the atomic number of the radiating particle.

The following table defines some of the terms normally used in radiation studies.

TABLE VI

DEFINITION OF TERMS

LET	linear energy transfer energy/unit length (ergs/cm) (The linear rate of loss of energy (locally absorbed) by an ionizing particle traversing a material medium.)
RBE	relative biological efficiency (The absorbed dose required to produce a given effect under gamma irradiation divided by the absorbed dose required to give the same effect when irradiation is by the particle being studied.)

TABLE VI (Continued)

rad	relative absorbed dosage energy/unit mass (100 ergs/gm) (The amount of energy imparted to matter by ionizing particles per unit mass of irradiated material at the place of interest.)
roentgen	energy/unit mass (83.8 ergs/gm or 0.93 rads) (The quantity of X, or gamma radiation, whose corpuscular emission per 1.293×10^{-3} gm of air (1 cm^3 of standard air) produces, in air, ions carrying one electrostatic unit of electricity of either sign.)
rep	roentgen-equivalent-physical energy/unit mass (93 ergs/gm) (Absorption of 93 ergs/gm of body tissue.)
rem	roentgen-equivalent-man energy/unit mass (The product of the dose in rads and RBE.)

The effects of secondary radiations should not be overlooked. In certain cases, the secondary emissions are more important than the primary radiation itself.

Energy is lost to a material by an impinging particle by one of two means, that is, either by absorption (where the energy is dissipated by the material as heat) or by scattering (where the energy is lost by a diffusing process with the material).

The secondary reactions occur from the interaction of the impinging electron on the exposed material. The individual atoms of the material absorb energy, and the orbiting electrons are excited into outer shells. The atoms then reradiate this energy in the form of electromagnetic radiation. Such a process is known as bremstrahlung. The resulting X-rays which are produced are extremely penetrating, and may initiate secondary radiations of their own.

Bremsstrahlung, an emission of very high energy electromagnetic radiation, requires several grams/cm^2 of shielding to absorb. The photons produced also initiate electron radiations by means of Compton scattering. If the photon is properly incident upon a loosely bound electron in the shielding material, it may impart a portion of its own energy to the electron. The photon also loses energy by the collision. The energy loss is proportional to the change in direction which the photon undergoes. This is the means by which X-rays are scattered.

X-rays are also absorbed by materials. The absorption coefficients depend upon the initial intensity of the X-rays and are given by

$$I = I_o e^{-\mu_\ell x}$$

where

I = the intensity of the radiation after passing through material thickness

I_o = initial photon intensity

μ_ℓ = linear absorption coefficient

x = thickness of the shielding material.

Values for μ_ℓ are given in Table VII for water, aluminum, iron, and lead.

TABLE VII

Wavelength Å	Photon Energy (Mev)	Typical Values f>			
		H_2O	Al.	Iron	Pb.
.062	0.20	0.133	0.360	.06	5.0
.025	0.50	0.096	0.[illegible]	.63	1.60
.012	1.00	0.071	0.168	.44	0.79
.009	1.50	0.057	0.136	.40	0.59
.006	2.00	0.050	0.117	.33	0.504

For the purposes of this report, we will overlook such things as pair production which occurs more in elements of high atomic number, since we do not expect to use these materials as prime shielding.

The mass absorption coefficient μ_m is found directly from the linear absorption coefficient μ_ℓ by the relation

$$\mu_m = \frac{\mu_\ell}{\rho}$$

where ρ is the material density.

A further consideration which must be taken into account is the scattering of high energy particles. From most experimental data only beam attenuation is considered, and the particles which are lost from the beam are assumed to have been absorbed. In many cases, the particles are dispersed and are lost to the beam, but must still be considered in shielding considerations.

Presently, vehicle configuration and vehicle material selections are made first, and the shielding calculations are then performed using these restrictions. For the problems which are of most concern in our primary attempts at manned space flight, this is probably an appropriate approach to the problem. It is to be hoped, however, that after we have passed through this embryonic stage, we will be able to give more consideration to vehicle configuration and material selections from a radiation standpoint. For instance, from a radiation point of view, a spacecraft might be better protected if it were laminated with a second material rather than the one material. It might be found even better to have several layers of different materials used in the construction of the vehicle. Still, a third alternative would be to construct a heavily shielded area within the confines of a lightly shielded vehicle, which personnel could enter in the event of a solar flare.

When one performs a radiation analysis upon objects located behind shields of different shapes, one finds that the amount of radiation incident upon the test object varies even though the initial ionizing intensity and shield thickness remains constant. Undoubtedly, there is an optimum vehicle configuration which would provide maximum shielding for any given enclosed volume.

It has also been found that the amount of radiation acquired by an object within a shielded volume is dependent upon the location of the object. The most desirable situation would be one in which the radiation was evenly distributed within the enclosed volume. An analysis of the radiation environment within a vehicle should consider this factor in vehicle configuration studies.

Finally, it is obvious from the foregoing discussion that much remains to be learned about the effects of radiation on human organs as well as the most effective shielding designs.

VI. CONCLUSIONS

Future studies should be concentrated on the following:

1. Studying the solar "surface" to determine the mechanisms involved in the solar atmospheric phenomena.
2. Analysis of the solar flare occurrences during the upcoming solar cycle to determine causes of solar flares.
3. Continued development and perfection of solar flare predicting techniques.
4. Development of the most effective solar flare shield which would be compatible with other considerations for selection optimum materials to be used in vehicle design.

Thorough solutions of these suggested points, especially 2 and 4, would result in a much more secure space program during the 1970's.

REFERENCES AND BIBLIOGRAPHY

1. Shulte, H. J., and E. N. Shipley, "Models for Space Environmental Hazards: Radiation," Bellcomm, Inc., Washington, D. C., January 31, 1964.
2. Webber, William R., "An Evaluation of the Radiation Hazard Due to Solar Particle Events," The Boeing Company, Document No. D2-90469, Seattle, Washington, November 12, 1963.
3. Freier, Phyllis, and William R. Webber, "Radiation Hazard in Space from Solar Particles," Science, Vol. 142, December 20, 1963.
4. Beckers, J. M., "A Study of the Fine Structures in the Solar Corona," AFCRL-64-770, Sacramento Peak Observatory, Air Force Cambridge Research Laboratories, September 1964.
5. Smith, H. J., "Solar Perturbations of the Space Environment," Second Symposium on Protection Against Radiations in Space, Gatlinburg, Tennessee, October 12-14, 1964.
6. Guss, Donald E., "Distribution in Heliographic Longitude of Flares which Produce Energetic Solar Particles," Physical Review Letters, Volume 13, No. 12, September 21, 1964.
7. Beck, Andrew J., and Edward L. Divita, "Evaluation of Space Radiation Doses Received Within a Typical Spacecraft," ARS Journal, November 1962.
8. Kuiper, Gerard P., Editor, The Solar System, Volume I, "The Sun," The University of Chicago Press, Chicago, Illinois, 1952.
9. Vosteen, Louis F., "Environmental Problems of Space Flight Structures: I. Ionizing Radiation in Space and Its Influence on Spacecraft Design," NASA TN D-1474, Langley Research Center, Hampton, Virginia, October 1962.
10. Schulte, H. J., "Apollo Mission Analysis for Radiation," Bellcomm, Inc., Washington, D. C., April 17, 1964.
11. Fuelsche, Trutz, "Estimates of Radiation Doses in Space on the Basis of Current Data," NASA, Langley Research Center, Hampton, Virginia, Life Science and Space Research, 1963.
12. Smith, Henry J., and Elske v. P. Smith, Solar Flares, The Macmillan Company, New York, 1963.

13. Le Galley, Donald P., Space Science, John Wiley and Sons, Inc., New York, 1963.

14. Le Galley, Donald P. and Alan Rosen, Space Physics, John Wiley and Sons, Inc., New York, 1964.

15. Roberts, W. T., "Space Radiations: A Compilation and Discussion," MTP-AERO-64-4, George C. Marshall Space Flight Center, Huntsville, Alabama, January 21, 1964.

16. Burrell, M. O. and J. W. Watts, "Flare Proton Doses Inside Lunar Structures," Internal Note R-RP-IN-64-16, George C. Marshall Space Flight Center, Huntsville, Alabama, May 22, 1964.

17. Madey, Richard, "Shielding Against Space Radiation," Nucleonics, Volume 21, No. 5, May 1963.

18. McDonald, Frank B., "Solar Proton Manual," NASA TR R-169, Washington, D. C., September 1963.

19. Tobias, Paul, "The Effects of Radiation on Integration Behavior," University of Southern California, Los Angeles, California, Spring 1962.

20. Keller, J. Warren, "The Shielding of Space Vehicles," NASA MTP-M-RP-61-12, George C. Marshall Space Flight Center, Huntsville, Alabama, May 16, 1961.

21. Fortney, Robert E. and Mae R. Morrison, "Radiation Hazards in Space," presented at AMD/ASD conference on "Crew Escape Techniques for Aerospace Vehicles," Wright Patterson Air Force Base, February 19-20, 1963.

22. Freier, P. S. and W. R. Webber, "Exponential Rigidity Spectrums for Solar-Flare Cosmic Rays," Journal of Geophysical Research, Volume 68, No. 6, March 15, 1963.

23. Madey, Richard, Arthur G. Duneer, Jr., and Theodore J. Kreiger, "Proton Dose Rates in Manned Space Vehicles," Preprint 62-22, American Astronautical Society, Eighth Annual National Meeting, January 16-18, 1962.

24. Madey, Richard, "A Current Survey of Space Radiation Hazards to Astronauts," Preprint 62-15, American Astronautical Society, Eighth Annual National Meeting, January 16-18, 1962.

25. Evans, Titus C., "Radiation Hazards of Space Exploration and Radiobiological Principles Involved," American Rocket Society/Oak Ridge National Laboratory, Space-Nuclear Conference, Gatlinburg, Tennessee, May 3-5, 1961.

26. Russak, Sidney L., "Radiation Shielding Considerations in Manned Spacecraft Design," Journal of Spacecraft, Volume 1, No. 3, May-June 1964.

27. Hildebrand, Robert I., "Energetic Particle Radiation in Space," NASA Lewis Research Center, Cleveland, Ohio, 1963.

28. Schaefer, Hermann J., "Tissue Ionization Dosages in Proton Radiation Fields in Space," Aerospace Medicine, October 1960.

29. Baker, Robert H., An Introduction to Astronomy, Van Nostrand Company, Inc., New York 18, New York, August 1961.

30. Goldberg, Leo, Annual Review of Astronomy and Astrophysics, Volume 1, Annual Reviews, Inc., Palo Alto, California, 1963.

31. Bailey, D. K., "Time Variations of the Energy Spectrum of Solar Cosmic Rays in Relation to the Radiation Hazard in Space," Journal of Geophysical Research, Volume 67, No. 1, January 1962.

32. Chapman, M. C. and M. R. Morrison, "A Summary of Natural Particulate Radiation in Space," Technical Documentary Report ASD-TDR-62-606, Wright-Patterson Air Force Base, Ohio, January 1963.

33. "Goddard Contributions to the 1963 Jaipur Conference on Cosmic Rays," Goddard Space Flight Center, Greenbelt, Maryland, March 1964.

34. Dalton, Charles C., "Estimation of Tolerance Limits for Meteoroid Hazard to Space Vehicles 100-500 Kilometers Above the Surface of the Earth," NASA TN D-1996, George C. Marshall Space Flight Center, Huntsville, Alabama, February 1964.

35. Anderson, Kinsey A., "Preliminary Study of Prediction Aspects of Solar Cosmic Ray Events," NASA TN D-700, Washington, D. C., April 1961.

36. Price, B. T., C. C. Horton, and K. T. Spinney, Radiation Shielding, Pergamon Press, New York, 1957.

37. Lapp, R. E. and H. L. Andrews, Nuclear Radiation Physics, Prentice-Hall, Inc., Englewood Cliffs, New Jersey, 1961.

REFERENCES AND BIBLIOGRAPHY (Continued)

38. Smith, Robert E., editor, "Space Environment Criteria Guidelines for Use in Space Vehicle Development," NASA TM X-53142, George C. Marshall Space Flight Center, Huntsville, Alabama, September 30, 1964.

39. Burrell, Martin O., "Space Radiation Doses During Planetary Missions," NASA TM X-53190, George C. Marshall Space Flight Center, Huntsville, Alabama, January 20, 1965.

THE SOLAR FLARE ENVIRONMENT

By W. T. Roberts

The information in this report has been reviewed for security classification. Review of any information concerning Department of Defense or Atomic Energy Commission programs has been made by the MSFC Security Classification Officer. This report, in its entirety, has been determined to be unclassified.

This document has also been reviewed and approved for technical accuracy.

Robert E. Smith
Robert E. Smith
Chief, Space Environment Group

W. W. Vaughan
Chief, Aerospace Environment Office

E. D. Geissler
Director, Aero-Astrodynamics Laboratory